



Giani, G., Rico-Ramirez, M. A., & Woods, R. A. (Accepted/In press). A Practical, Objective and Robust Technique to Directly Estimate Catchment Response Time. *Water Resources Research*, 57(2), [e2020WR028201]. <https://doi.org/10.1029/2020WR028201>

Peer reviewed version

Link to published version (if available):
[10.1029/2020WR028201](https://doi.org/10.1029/2020WR028201)

[Link to publication record in Explore Bristol Research](#)
PDF-document

This is the author accepted manuscript (AAM). The final published version (version of record) is available online via Wiley at <https://doi.org/10.1029/2020WR028201>. Please refer to any applicable terms of use of the publisher.

University of Bristol - Explore Bristol Research

General rights

This document is made available in accordance with publisher policies. Please cite only the published version using the reference above. Full terms of use are available: <http://www.bristol.ac.uk/red/research-policy/pure/user-guides/ebr-terms/>

13 Abstract

14 Methodologies to estimate the response time of a catchment to new rainfall inputs based on
15 rainfall and streamflow observations require the analyst to make a number of uncertain and
16 subjective steps. Moreover, these methods make the assumption that the water producing the
17 discharge peak fell in the last rainfall event, which does not necessary apply to all the
18 environments and conditions. Hence, here we present a practical, objective, and robust
19 method to estimate catchment response time (T_r) based on hourly rainfall and streamflow
20 time series only, which removes most of the sources of uncertainties arising from current
21 methodologies by restating the conceptual hypothesis and minimizing the user's choices. The
22 proposed method, used originally in the field of economics to assess the temporal correlation
23 between two variables, has been adapted to be used for the first time in the field of
24 hydrology. The method does not make any assumption about the rainfall-runoff
25 transformation (no hydrograph separation needed), does not require event selection or
26 parameter estimation, and it is easily reproducible. The above features make the proposed
27 method a useful tool even under different hypothesis regarding the hydrograph water age.
28 The method agrees well with the traditionally used method to estimate T_r from observed
29 hyetographs and hydrographs (Spearman rank correlation $r=0.82$). The proposed method
30 gives robust results for relatively short records, and works in presence of noise and bias in the
31 time series.

32 Plain language summary

33 Methodologies to estimate the time delay of the transformation of rainfall into river discharge
34 based on rainfall and discharge records require a number of highly subjective and uncertain
35 steps. Moreover, the assumptions behind these methods have been proven incorrect, at least
36 in some environments. For this reason, we present a different method which removes those
37 incorrect assumptions and most of the sources of uncertainties arising from the other
38 methodologies. Unlike existing methods, the proposed methodology does not make any
39 assumption about the processes that transform rainfall into river discharge, does not require
40 event identification or parameter estimation and is easily reproducible. We demonstrate that
41 the new approach compares well with the traditionally used method and also works for short
42 and noisy records.

43 1.Introduction*44 The need for a new method*

45 The fast response time of a catchment to new rainfall inputs is one of the key time variables
46 in hydrology (Kibler, 1982; Almeida et al., 2014) and its correct estimation is essential for
47 hydrological modelling and hydrograph design. Uncertainty in its estimation can cause errors
48 in estimation of peak discharge rate and timing of flood events (Perdikaris et al., 2018).

49 McCuen (2009) summarised the estimation procedures for determining this response time
50 using rainfall and streamflow observations. These methodologies are straightforward in
51 transferring theoretical knowledge to an estimation procedure, as they estimate a time
52 parameter using a computational definition. Two of the most commonly used definitions
53 when applying these methods are (McCuen, 2009):

54 1. The time from end of rainfall excess to the inflection point in the hydrograph falling limb;

55 2.The time from centre of mass of rainfall excess to centre of mass of direct runoff (also
56 called time lag).

57 The first definition is the most traditionally used when applying these methods, but it has
58 been demonstrated to be highly uncertain (McCuen, 2009) as it involves identifying the
59 precise times of individual features of hyetograph and hydrograph. The second definition,
60 involving centres of mass, is more robust as averaging accounts for the overall behaviour of
61 the rainfall excess and direct runoff (McCuen, 2009). However, since it is the most
62 traditionally applied, in this work we will consider the first definition and will refer to related
63 estimation procedure as “traditional method”.

64 Nevertheless, applying any of these definitions to estimate the response of the catchment to
65 new rainfall input requires the analyst to take a number of highly uncertain and subjective
66 steps:

- 67 • Identification of rainfall-streamflow events: there is no recognized and standardized
68 methodology in the literature to automate the selection of rainfall-streamflow events
69 (Norbiato et al., 2009; Merz & Blöschl, 2009; Tarasova et al., 2018; Mei &
70 Anagnostou, 2015) and the chosen strategy has an impact on rainfall (Dunkerley,
71 2008) and therefore presumably on streamflow statistics at the event scale.
72 Furthermore, the type and the number of the storm events taken into account can
73 affect the response time of a catchment (Grimaldi et al., 2012).
- 74 • Separation of the hydrograph into direct runoff and baseflow: many automated
75 methods for hydrograph separation use recursive one-parameter digital filters (e.g.
76 Lyne & Hollick, 1979, Nathan & McMathon, 1990), but these methods require the
77 estimation of a parameter which lacks a physical meaning. Other, more sophisticated
78 hydrograph separation methods usually involve multiple parameters (e.g. two
79 parameter filter by Eckhardt, 2005), which makes parameter estimation more
80 complicated and uncertain.
- 81 • Identifying the time of occurrence of hyetograph and hydrograph features: the noise in
82 the signals can make it difficult to automatically identify these features (e.g. inflection
83 points in the hydrograph), especially when the temporal resolution of the data is high.

84 Furthermore, recently, tracer studies (e.g. McDonnell, 1990; Berghuijs & Allen, 2019; Gallart
85 et al., 2020) have highlighted how in some environments the storm hydrograph mainly
86 consists of water that fell in previous rainfall events. Thus, for some environments there are
87 clear conceptual weaknesses in the methods summarized by McCuen (2009) as they are
88 mainly based on the concept of runoff event made of water falling in the last rainfall event.

89 To overcome these limitations, we propose a practical, objective, and robust methodology to
90 directly estimate the fast response of the catchment to new rainfall input using rainfall and
91 streamflow observations. The resulting estimates are conceptually similar to the ones
92 produced by the methods summarized by McCuen (2009), but they express the average time
93 delay between centre of mass of total hyetograph and centre of mass of the corresponding
94 total hydrograph. In particular, the proposed methodology improves upon the existing
95 methods with the following advantages: (a) it makes no assumptions on the rainfall-runoff
96 transformation; (b) there is no need of rainfall-streamflow event selection or hydrograph
97 separation; (c) it requires no parameter estimation; and (d) it is easily reproduced.

98 We will call the time estimated by the traditional method and the proposed method the
99 “catchment response time” (T_r). The following subsection outlines our reasoning for this.

100 *A Note on Definitions and Terminology*

101 The term “time of concentration” (T_c) is frequently used in quantifying the flow response to
102 rainfall events, but it is unsuitable to describe the method presented in this paper. Often, this
103 terminology is stretched to include estimates coming from methods with very different
104 conceptual hypotheses (Grimaldi et al., 2012), but this can generate confusion and murkiness
105 around the concept of T_c .

106 T_c is historically defined as the time after initiation of steady rainfall when storage is no
107 longer increasing. For example, storage may refer to surface detention storage (e.g. Luce and
108 Cundy, 1994) or to water stored in an equilibrium flow profile (Henderson and Wooding,
109 1964). T_c can also be associated with the concept of time to equilibrium (the time from the
110 start of rainfall to peak response) in the case of dry initial conditions and steady input rainfall
111 (Eagleson, 1970).

112 Confusingly, the International Glossary of Hydrology defines T_c as the time for the storm
113 runoff to flow from the most hydraulically distant point in the catchment to the catchment
114 outlet (W.M.O., 1974; Johansson, 1984). As pointed by Beven (2020), this definition is in
115 contradiction with historical one as it assumes that the water moves as individual particles
116 and not as a wave. Beven (2020) also states that we should abandon the glossary definition
117 and that the concept of velocity of water particles should be replaced by the wave celerity
118 concept, given the fact that water moves as a wave.

119 Being consistent with the historical definition of T_c when using the terminology “time of
120 concentration” is of paramount importance. In fact, the historical T_c concept is used in
121 engineering applications, especially for small drainage areas, as critical duration (duration of
122 the uniform precipitation for which we observe the maximum discharge) (USDA-NRCS,
123 2010). Calling estimates coming from methods with different conceptual hypotheses “time of
124 concentration” can generate confusion and potentially could lead to substantial errors in the
125 engineering applications.

126 Nonetheless, the assumption of steady rainfall behind the historical definition of T_c might not
127 apply to the majority of rainfall events in the real world, especially with larger drainage areas.
128 Hence, the time scale retrieved using methods which follow the historical definition may not
129 reflect the most typical response time of the catchment. Instead, simultaneous measurements
130 of catchment rainfall and streamflow provide evidence of the real-world response time.

131 McCuen (2009) summarised methods for determining a response time for catchments with
132 rainfall and streamflow observations and he called the resulting time estimates “time of
133 concentration”. However, the conceptual basis of hyetograph-hydrograph analysis is
134 inconsistent with the historical definition of T_c , and a different term is needed. For this
135 reason we instead use the term “catchment response time”, T_r , for the time derived using the
136 traditional method and the method proposed in this paper.

137

138

139 2.Methodology

140 2.1. DMCA-based correlation-coefficient methodology

141 The proposed methodology to directly estimate Tr from rainfall and streamflow observations
 142 is based on the Detrending Moving-average Cross-correlation Analysis (DMCA). This
 143 technique was developed in economics to understand the time scale at which two variables
 144 are most strongly correlated (Kristoufek, 2014; Kristoufek, 2015). To the best of our
 145 knowledge it has not yet been applied in hydrology. The Tr estimate calculated with the
 146 DMCA-based method characterises the time scale of the transformation from a noisy rainfall
 147 input to a smoother streamflow output at the catchment outlet.

148 The strength of the DMCA-based method is to find the timescale at which two time series are
 149 linked even when they exhibit different frequency spectra and are nonlinearly related. If we
 150 simply used cross correlation by itself, prior smoothing of the rainfall time series would be
 151 required to ensure it had a similar frequency to that of the streamflow series. This smoothing
 152 would alter the structure of the input rainfall signal, ultimately leading to errors when
 153 calculating the timescale of the catchment response.

154 We adapted the DMCA methodology to extract an average estimate of Tr from rainfall-
 155 streamflow time series containing multiple events. Although the hypothesis of quasi-invariant
 156 Tr can be verified only for events with high return periods (Dooge, 1973), an invariant
 157 estimate of Tr for each catchment is often useful to characterise the catchment and that's what
 158 our proposed method does.

159 In section 2.1.1 we present the analytical formulae and in section 2.1.2 we show the
 160 reasoning behind each step. The DMCA-based method can also be applied at event scale by
 161 using a time series created by concatenating copies of the same event. This requires a few
 162 adjustments which are presented in section 2.1.3.

163 2.1.1 Step by step guide to DMCA calculations

164 Here we outline the steps for calculating Tr using mean catchment rainfall and streamflow
 165 time series (typically at hourly time step):

166 I. Construct the cumulative time series of rainfall R_t and streamflow Q_t . The two time
 167 series must have the same length T and the same time step:

$$168 \quad R_t = \sum_{i=1}^t r_i \quad \text{for } t=1,2,\dots,T \quad (\text{Eq.1})$$

$$169 \quad Q_t = \sum_{i=1}^t q_i \quad \text{for } t=1,2,\dots,T \quad (\text{Eq.2})$$

170 Where r_i and q_i are the rainfall and the streamflow records respectively at time t and
 171 R_t and Q_t are the cumulative time series for time series of length T .

172 Then, for a single moving-average window length L (where L is in units of time steps and
 173 must be odd as we are using centred moving average):

174 II. Calculate the fluctuations of each cumulative time series compared to its centred
 175 moving average (this is the detrending) with window length L , and then compute the
 176 mean squared value of those fluctuations ($F_R^2(L)$ for rainfall and $F_Q^2(L)$ for
 177 streamflow):

$$178 \quad F_R^2(L) = \frac{1}{T-L+1} \sum_{t=0.5(L+1)}^{T-0.5(L-1)} (R_t - \widehat{R}_{t,L})^2 \quad (\text{Eq.3})$$

179
$$F_Q^2(L) = \frac{1}{T-L+1} \sum_{t=0.5(L+1)}^{T-0.5(L-1)} (Q_t - \widehat{Q}_{t,L})^2 \quad (\text{Eq.4})$$

180 Where $\widehat{R}_{t,L}$ and $\widehat{Q}_{t,L}$ are the centred moving averages of the cumulative rainfall and
 181 streamflow respectively with moving average window length L at time t :

182
$$\widehat{R}_{t,L} = \frac{1}{L} \sum_{t-0.5(L-1)}^{t+0.5(L-1)} R_t \quad (\text{Eq.5})$$

183
$$\widehat{Q}_{t,L} = \frac{1}{L} \sum_{t-0.5(L-1)}^{t+0.5(L-1)} Q_t \quad (\text{Eq.6})$$

184 III. In the same way, calculate the mean squared value of the bivariate fluctuations:

185
$$F_{R,Q}^2(L) = \frac{1}{T-L+1} \sum_{t=0.5(L+1)}^{T-0.5(L-1)} (R_t - \widehat{R}_{t,L})(Q_t - \widehat{Q}_{t,L}) \quad (\text{Eq.7})$$

186 IV. Finally, the DMCA-based correlation coefficient for a window length L is:

187
$$\rho_{DMCA}(L) = \frac{F_{R,Q}^2(L)}{F_R(L)F_Q(L)} \quad \text{with } -1 \leq \rho_{DMCA}(L) \leq 1 \quad (\text{Eq.8})$$

188 Tr is estimated as half of $L_{\min}-1$, where L_{\min} is the window length L which gives the minimum
 189 value of the DMCA-based correlation coefficient ρ_{DMCA} . We therefore need to test a wide
 190 range of window lengths L , from three hours to several days using a two-hour time step (to
 191 ensure that L is an odd number) so that we are sure to include the window associated to Tr for
 192 the analysed catchment. Python and Matlab functions to estimate Tr using DMCA-based
 193 method are available at https://github.com/giuliagiani/Tr_DMCA, last access 11.09.2020.

194 Previous application of steps I to IV in economics aimed to understand if two variables were
 195 correlated at short, medium or long time scales. The window length L of maximum absolute
 196 correlation between the two variables provided an estimate of this time scale (Kristoufek,
 197 2015). We instead reinterpret the results to get a numeric estimate of Tr as half the window
 198 length $L_{\min}-1$. Therefore, a further novelty of this work is that we are reinterpreting the output
 199 of the DMCA method, as well as applying it in a hydrological context for the first time.

200 The methodology is a time series analysis technique but does not necessarily require
 201 continuous records for robust Tr estimates. When missing values occur in the time series, the
 202 methodology will automatically estimate Tr using other periods of the record, hence reducing
 203 manual data pre-processing tasks. This is not valid if the data are highly intermittent (e.g. one
 204 hourly timestep missing every day) as, by breaking the time series too many times, the Tr
 205 estimate can be affected. For a robust Tr estimate the time series should include at least one
 206 section with no missing time steps longer than the longest moving average window length L
 207 tested.

208 **2.1.2 Interpretation of DMCA-based methodology**

209 This section explains the reasoning for steps I-IV above, and gives an explanation of how the
 210 window giving the minimum value of cross-correlation is related to Tr. To follow the
 211 explanation of the four steps, we refer to the first column of Figure 1 (Figures 1a-1c), where
 212 we graphically represent the steps for a single window length ($L=151$). The DMCA-based
 213 method has been applied to rainfall-streamflow time series but for simplicity in Figure 1 we
 214 zoom on an individual event so we can graphically explain in detail the meaning of the steps.

215 I. A new input will cause a sudden steepening in the cumulative time series (see
 216 comparison between Figures 1a-1b (solid lines)). In particular:

- 217 • For the cumulative rainfall time series, increases in cumulative rain correspond
 218 to new rainfall contributions while flat sections correspond to periods of zero
 219 rainfall (solid green line in Figure 1b).
 220 • For the cumulative streamflow time series, we can observe steeper increases in
 221 cumulative flow for the rising limb (new streamflow contribution) and flatter
 222 increases for recessions (solid grey line in Figure 1b).
 223
- 224 II. The moving average (dashed lines in Figure 1b) of the cumulative time series
 225 intersects the step change in its centre of mass at the window length scale, generating
 226 negative fluctuations (moving average series above cumulative time series) at the
 227 beginning of the contribution and positive fluctuations (moving average series below
 228 cumulative time series) at the end (see comparison between solid and dashed lines in
 229 Figure 1b).
 230 The points where fluctuations change from negative to positive (large dots in Figure
 231 1b) are physically meaningful: they correspond to the centre of mass of the
 232 contribution at the window length scale, which refers to centre of mass of rainfall and
 233 streamflow. For each rainfall-streamflow event the time interval between these two
 234 points can then be interpreted as T_r . One definition of T_r by McCuen (2009) is the
 235 time from the maximum rainfall intensity to the peak of discharge. For multi-peak
 236 events the maximum intensity/peak does not always provide sufficient information,
 237 hence we prefer the use of centres of mass. However, the next steps (III and IV) are
 238 required to estimate T_r , as knowing only the position of the centres of mass for each
 239 event would imply an independent estimate of T_r for each of them.
 240 At this stage for Equations 3 and 4 the sign of the fluctuations is not important as the
 241 fluctuations are squared. These two equations serve only as a measure of the
 242 magnitude of fluctuations, which will be used later to normalise bivariate fluctuations.
 243
- 244 III. Bivariate fluctuations (the product of rainfall and streamflow fluctuations) determine
 245 the sign of the DMCA-based correlation coefficient (Eq.8) as in the numerator (Eq.7)
 246 the sign of rainfall and streamflow fluctuations plays an important role.
 247 If streamflow would react instantaneously to rainfall and keep the same frequency
 248 spectrum, rainfall and streamflow at any time t would have the same fluctuation sign,
 249 i.e. both negative before the centre of mass and positive after it, resulting in positive
 250 bivariate fluctuations. Instead, every time a rainfall contribution occurs, streamflow
 251 responds with a certain delay and the signal is smoothed out. Therefore, when rainfall
 252 fluctuations are already positive because the rainfall centre of mass has passed,
 253 streamflow still shows negative fluctuations (it has not yet reached the streamflow
 254 centre of mass), causing negative bivariate fluctuations.
 255 Fig 1.c shows fluctuations of the individual rainfall and streamflow signals. The red
 256 arrow underlines the time period in which bivariate fluctuations are negative.
 257
- 258 IV. Bivariate fluctuations are then normalized by the product of the rainfall and
 259 streamflow fluctuations so that the correlation does not depend on the magnitude of
 260 the signals.
- 261 In Figures 1d-1i we can see the effects of different moving average window lengths, L .
 262 Firstly, we can see that fluctuation amplitudes and durations increase with increasing moving

263 average window lengths (Figures 1c, 1f and 1i), as a longer moving average window lengths
264 tend to smooth out more features of the original time series, generating bigger fluctuations.

265 Given that bivariate fluctuations are negative when streamflow is first responding, bivariate
266 fluctuations are maximized, producing a minimum in the DMCA-based correlation
267 coefficient, when both rainfall positive fluctuations and streamflow negative fluctuations are
268 covering the whole time span between the two centres of mass (between the two dots). This
269 happens only when using a moving-average window length which is double the time between
270 the two centres of mass, i.e. double the Tr (Figure 1e-1f). The factor two in the relationship
271 between Tr and window length is inherent to the centred moving average process, as to
272 generate a fluctuation of one sign for a specific duration, the window length has to be twice
273 as large. Note that the DMCA-based correlation coefficient value does not have a statistical
274 significance level because it is dependent on how many events occurred and on their
275 duration. However, when applying different moving-average window lengths to the same two
276 time series, the value of the DMCA-based correlation coefficient is able to guide us through
277 the estimation of Tr (Figure 1j).

278 Shorter window lengths (e.g. $L=151$, Figure 1c) generate negative bivariate fluctuations for a
279 time period shorter than the time span between the two centres of mass (red arrow shorter
280 than the time span between the dots). The DMCA-based correlation coefficient ρ_{DMCA} for a
281 window L of 151 is in fact smaller in absolute terms than the one for a window length of 273
282 (Figure 1j). Longer window lengths ($L=351$, Figure 1i), despite covering the entire time span
283 between the centres of mass (time span between the two dots), also produce a significant
284 portion of positive fluctuations (blue arrows). These positive fluctuations increase bivariate
285 fluctuations that, when normalised, result in a smaller in absolute terms value of DMCA-
286 based correlation coefficient (Figure 1j).

287 In Figure 1f we can see that before the rainfall centre of mass we also have a small portion of
288 positive bivariate fluctuations, but these are smaller than the loss of negative bivariate
289 fluctuations using a smaller window (e.g. $L=271$), so $L=273$ is the optimum. In this sense, Tr
290 estimates calculated with the DMCA-based method can suffer from small errors due to the
291 geometry of the integrated time series, but these are minimal and, when the data resolution is
292 adequate, smaller than the range of variability of Tr in an individual catchment.

293 If we think of negative fluctuations as rising limbs and positive fluctuations as recessions, the
294 moving-average window length associated with Tr is the one which is able to group together
295 rainfall contributions so that the rainfall "recession" is concurrent with the rising limb of
296 streamflow (see Figure 1f). It is equivalent to creating two triangular shapes in which the
297 second half of the rainfall triangle basis overlaps with first half of the streamflow triangle (i.e.
298 recession of rainfall overlapping with rising limb of streamflow).

299

300 **Figure 1:** a-i) Graphic representation of steps (I, II, III) of DMCA-based methodology for moving average window lengths $L=151$, $L=273$,
301 $L=351$. Green lines relate to rainfall, grey lines to streamflow. The red (blue) arrows underline periods of negative (positive) bivariate
302 fluctuations. j) DMCA-based correlation coefficient variability with L , with circles showing correlation for the three window lengths above.

303 2.1.3 Event scale application of DMCA-based methodology

304 The DMCA-based methodology has not been built to work on an event-basis but with a few
305 adjustments it is also able to produce estimates for individual events. This is of interest for
306 comparison with existing event-based methods.

307 If rainfall-runoff events have been selected (see Supporting Information), then for each
308 individual event we create two time series, one concatenating copies of the rainfall event, the
309 other concatenating copies of the related streamflow event. By creating these artificial
310 records we are able to use the method also at the event scale. The copies must be separated
311 with an array of constant values of the same length for both time series and longer than the
312 longest window amplitude tested. In this way, any rainfall contribution occurring after the
313 discharge peak will still be associated with its own copy and not with the following replicated
314 events.

315 Rainfall events are separated by an array of zero values, whilst the constant value used to
316 separate streamflow events is the last value of the streamflow event. However, it is possible
317 that the beginning and the end of the streamflow event assume different values. When we
318 concatenate the streamflow copies, this can generate step changes, which can alter the
319 estimate of the response time. For this reason, when using the DMCA-based method at event
320 scale, we take into account only those estimates of response time coming from events where
321 the difference between the streamflow value at the beginning and at the end of the streamflow
322 event is less than 10% of the magnitude of the peak.

323 2.2. Traditional method

324 Among the multiple definitions available in the literature, the one traditionally used to
325 directly estimate T_r from rainfall and streamflow time series defines T_r as the time from the
326 end of rainfall excess to the inflection point of the total storm hydrograph (McCuen, 2009).
327 This definition of course refers to an individual event. Despite its conceptual simplicity,
328 estimating the end of rainfall excess and the inflection points in the total storm hydrograph
329 and direct runoff can be very challenging (Grimaldi et al., 2012).

330 The first step is to estimate the volume of direct runoff by separating the hydrograph into
331 baseflow and direct runoff using a recursive digital filter (e.g. Lyne & Hollick, 1979; Nathan
332 & McMahon, 1990):

$$333 \quad Q_d(t) = \beta Q_d(t-1) + \frac{1+\beta}{2} [Q(t) - Q(t-1)] \quad (\text{Eq.9})$$

334 Where $Q(t)$ and $Q(t-1)$ are total storm streamflow at times t and $t-1$, $Q_d(t)$ and $Q_d(t-1)$ are
335 direct streamflow at times t and $t-1$ and β is the recursive filter parameter.

336 The filter is applied three times (forward-backward-forward) to minimize the shift in time of
337 the output caused by the filtering process (Nathan & McMahon, 1990). The parameter β is
338 estimated so that the baseflow hydrograph passes through the inflection point of the total
339 storm hydrograph.

340 Many alternative methods are available for baseflow separation but they all suffer from
341 significant uncertainties, as they involve parameter estimations which do not have an
342 independent physical meaning (e.g. Sloto & Crouse, 1996; Lyne & Hollick, 1979; Furey &
343 Gupta, 2001; Eckhardt, 2005). Unless experiments with tracers or groundwater measurements

344 have been conducted in the examined catchment, the absence of a “true” baseflow makes the
345 objective evaluation of the different methods impossible (Eckhardt, 2008).

346 The end of rainfall excess is computed using the Soil Conservation Service Curve Number
347 (SCS-CN) method (USDA-SCS, 1986; Chow et al., 1988) in which the CN (Curve Number)
348 is estimated by assuming that the volume of excess rainfall is equal to the volume of direct
349 runoff. However, this methodology can sometimes lead to unrealistic estimates of T_r : this is
350 the case when close to the end of a rainfall event rainfall is falling at very low intensity.
351 Because of the previous rainfall which presumably saturated the soil, this low intensity
352 rainfall falling just after is considered excess rainfall moving forward in time to the end of the
353 rainfall excess. This leads to very short T_r estimates, which in some cases can even become
354 negative (Figure 2). More specifically, when using the traditional method in this paper, a
355 rainfall event was discarded if the total rainfall in the last three hours of the event was smaller
356 than three times the average rainfall rate for the whole event, or less.

357

358 **Figure 2:** Example of an event (catchment ID: 41025) which has been discarded due to the
359 long tail in the rainfall record (crosses represent end of rainfall excess (top) and inflection
360 point in the hydrograph (bottom)).

361 2.3. Lag estimate from Flood Estimation Handbook

362 In this work we used an estimate of response time retrieved from catchment descriptors to
363 guide the event selection (see Supporting Information) and to discuss any large difference
364 between T_r estimates from DMCA-based method and traditional method. Although rainfall
365 and streamflow records are available, the idea is to calculate an estimate of response time
366 which is independent from any direct observation from the data, using established methods.

367 In particular, in the Flood Estimation Handbook (FEH - Snyder, 1938; Houghton-Carr, 2008)
368 the lag is defined as the time from the centroid of total rainfall to the runoff peak or centroid
369 of runoff peaks. This definition is similar to the ones adopted by the other methods applied in
370 this work to describe T_r . However, this is not surprising as McCuen (2009) highlighted that
371 there is sometimes overlap in the definition of T_r and time lag.

372 Taking information from the FEH (Houghton-Carr, 2008), we estimate time to peak T_{p0}
373 using catchment descriptors (Equation 10) and then from the time to peak we derive the lag
374 (LAG) using an empirical formula (Equation 11). These empirical relationships are valid for
375 UK catchments only:

$$376 \quad T_{p0} = 1.684 \text{ DPSBAR}^{-0.18} \text{ PROPWET}^{-1.05} \text{ DPLBAR}^{0.48} (1 + \text{URBEXT})^{-4.39} \text{ [h]} \quad (\text{Eq. 10})$$

$$377 \quad LAG = \left(\frac{T_{p0}}{0.879} \right)^{1.05} \text{ [h]} \quad (\text{Eq. 11})$$

378 Where DPSBAR is the Drainage Path Slope [m km^{-1}], PROPWET is the proportion of time
379 soils are wet [-], DPLBAR characterizes catchment size and configuration [km] and
380 URBEXT is the urban extent [-]. For all the catchments for which the descriptors were
381 available, lag estimates are reported in Table S1.

382

383 3. Study catchments and data

384 We compare the DMCA-based method with the traditional method in a subset of catchments
 385 from the UK's National River Flow Archive (NRFA). We use catchments from the UK
 386 Benchmark Network 2 (UKBN2) which have been classified as near-natural (Harrigan et
 387 al.,2018). We will make use of this set of near-natural catchments to test the proposed
 388 methodology without adding more complexity due to human disturbance.

389 Mean areal hourly rainfall has been derived from the continuous CEH-GEAR1hr dataset for
 390 each catchment (Lewis et al., 2018). Streamflow data at 15-min step were provided by the
 391 Environmental Agency (EA), Natural Resources Wales (NWR) and Scottish Environmental
 392 Protection Agency (SEPA) and then processed to obtain hourly streamflow time series. The
 393 percentage of missing values in the available streamflow records varies from 0 to 60% with a
 394 median value of 0.2%. We did not discard the catchments with higher percentages of missing
 395 values as the other parts of the records were long enough to compute reliable estimates of T_r .

396 Rainfall and streamflow time series at hourly resolution were available for only 113 out of
 397 146 catchments. Base Flow Index (BFI) is provided for catchments in the UKBN2, and to
 398 guarantee a fast hydrograph response we excluded catchments with very large BFI (> 0.85).
 399 This reduced the catchment study set to 98 of the 146 catchments of UKBN2 (see Figure 3,
 400 all markers), with areas ranging from 8 to 1508 km². For these catchments, the record length
 401 for which both hourly rainfall and streamflow data are available varies from 17 to 24 years.

402 Since the traditional method can only be used on an event basis, we need to select individual
 403 rainfall-streamflow events from the continuous time series. To do so, we used the
 404 methodology outlined in Supporting Information which involves the use of catchment
 405 descriptors. Taking information from the UK hydrometric Register (Marsh & Hannaford,
 406 2008) and Flood Estimation Handbook (FEH) (Bayliss, 2008), the descriptors were only
 407 available in 79 of the 98 basins. However only for 76 catchments, it was possible to find a set
 408 of events which were suitable for the application both of DMCA method and traditional
 409 method. Therefore, the evaluation of DMCA method against the traditional method (Sections
 410 4.1 and 4.2 and Figures 4) is further restricted to just these 76 catchments (Figure 3, see
 411 catchments represented with a blue asterisks), while the robustness analysis of DMCA
 412 (Section 4.3 and Figures 6) is performed on the 98 catchments (Figure 3, see all catchments)
 413 as no event selection is needed.

414

415 **Figure 3:** Locations of the 98 study catchment outlets with their National River Flow Archive
 416 identification number (orange circles show catchments used only for robustness analysis
 417 (Section 4.3), blue asterisks show catchments used both for evaluation (Sections 4.1,4.2) and
 418 robustness analysis (Section 4.3)).

419 4.Results

420 4.1. Event-based comparison: does the median value of the T_r distribution with DMCA- 421 based methodology match the median from the traditional method?

422 As mentioned in the methodology section, both the DMCA-based method at event scale and
 423 the traditional method are unable to provide reliable estimates of T_r for some types of events.
 424 Hence, we introduced a discarding rule for each method. After selecting the rainfall-

425 streamflow events (see Supporting Information), we compared the two methodologies in each
 426 catchment considering only the events for which both Tr estimates were available. As a
 427 result, in each catchment we produced two Tr sample distributions, one for each method,
 428 based on the same set of events.

429 The number of events for which Tr estimates are available with both methodologies ranges
 430 from 1 to 183 events with a median value of 21 events across the different catchments. These
 431 numbers come from the intersection of the Tr estimates from the traditional method (number
 432 of events ranges from 5 to 685 with a median of 63 events) and the estimates from the
 433 DMCA-based methodology at event scale (number of events ranges from 27 to 816 with a
 434 median of 178 events).

435 In Figure 4a we compare Tr estimates from the DMCA-based method and traditional method
 436 performed on an event basis. Each catchment is represented by a circle showing the median
 437 Tr estimate when using both methodologies across all of the considered events, with the bars
 438 then highlighting the 25th and 75th percentiles. Blue and red colours stand respectively for
 439 sample larger/equal and smaller than 10 events, as small samples of events might lead to less
 440 robust estimate of Tr.

441 Overall, we can see that the median values (circles in Figure 4a) of the two Tr distributions
 442 derived with two methodologies are mostly on a 1:1 line (Spearman rank correlation equal to
 443 0.82). This indicates that DMCA-based method produces results which are generally similar
 444 to the traditional method.

445 **4.2. When using DMCA-based methodology, does the Tr estimate from the analysis of** 446 **the entire time series match the median of the estimates from individual events?**

447 In the previous section we used the DMCA-based methodology for individual events and the
 448 results were compared with the traditional method. However, as mentioned in the
 449 methodology section, the DMCA-based method was originally developed to analyse the
 450 entire time series and not just on an event basis. The aim is to find an average Tr for the
 451 whole record.

452 Hence, we applied the DMCA method for estimating on both an event basis and across the
 453 entire rainfall and streamflow time series. We compared the Tr estimate from across the
 454 entire time series to the median Tr estimate of the individual events (Figure 4b). We use
 455 color-coding to distinguish those catchments whose median is based on an event sample
 456 smaller or larger than 10 events.

457 The median value of the Tr distribution using DMCA-based methodology for individual
 458 events compares well with the Tr estimate on the entire time series (Spearman rank
 459 correlation equal to 0.94), showing that the process of event identification is not needed when
 460 using the DMCA-based method.

461

462 **Figure 4:** a) Median, 25th and 75th percentiles of times of concentration distributions for each
 463 catchment using the traditional method and the DMCA-based method. Capital letters refers to
 464 catchments mentioned in the Section 5.1. b) Comparison of application of DMCA-based
 465 methodology on the entire time series with median of Tr distributions of individual events. In

466 both plots catchments in red (blue) highlights catchments where less than (more than or equal
467 to) 10 independent events were identified. Note logarithmic scales.

468 **4.3. How sensitive is the DMCA-based methodology to the length of the record and to**
469 **noise and bias in the time series?**

470 As a first test, we evaluate the robustness of our proposed methodology for shorter records. In
471 each catchment we break down the original time series in two calendar year sub-dataset and
472 for each of them we computed the T_r using the DMCA-methodology (e.g. for an original
473 rainfall-streamflow record from 1990 to 2010, the two-calendar-year sub-datasets are 1999-
474 2000, 2000-2001, ..., 2009-2010). In Figure 5a we show with a blue bar the minimum-
475 maximum range of T_r estimates obtained with all the two-year datasets in each of the 98
476 catchments. The star represents the T_r using the whole available record length, which ranges
477 from 17 to 24 years in different catchments. We repeated the same procedure for sub-datasets
478 of 5 and 10 years (Figure 5b and 5c).

479 The results show that the DMCA-based methodology can produce robust estimates even with
480 relatively short rainfall-streamflow records. Figure 5a shows that for catchments responding
481 in less than 10 hours a two-year record of hourly data is already long enough to robustly
482 estimate T_r , as shown by the minimum and maximum values converging towards the estimate
483 from analysing the time series as a whole. Catchments responding in 10-20 hours require
484 longer time series with at least 5 years of hourly data. In catchments where the response time
485 is greater than 20 hours, at least 10 years of hourly data are needed for robust estimates.
486 Therefore, according to our DCMA methodology, the record length of hourly data needed for
487 robust T_r estimation increases with increasing response times of the catchment.

488

489 **Figure 5:** Tr estimates using subsets of 2(a), 5(b), 10(c) years (blue bars). The triangle represents the Tr estimate using the entire record. Where
490 no bar is visible, the range of estimates was smaller than the width of symbol.

491 Our second test evaluates the robustness of the methodology when time series are affected by
492 noise. We add random Gaussian noise to rainfall and streamflow time series with standard
493 deviations of 5% and 25% of the mean value, respectively green stars and orange circles in
494 Figure 6a. This means that 98% of the data points increase or decrease their values by 0-10%
495 of the mean value, when the standard deviation is equal to 5% of the mean, and by 0-50% of
496 the mean when the standard deviation is 25% of the mean. We then compare Tr estimates
497 from the perturbed and original time series (respectively green stars/orange circles and black
498 triangles in Figure 6a), applying the DMCA method across the entire length of each of the
499 records.

500 Results show that adding noise to the original streamflow record has a minimal effect on the
501 Tr estimates computed with the DMCA-based methodology. Only 4 out 98 catchments show
502 variations in Tr estimate when Gaussian noise with standard deviation of 5% of the mean is
503 added to the original rainfall and streamflow time series (green stars in Figure 6a). The
504 average error is less than 1%. When the standard deviation of the Gaussian noise increases to
505 25% of the mean value, 33 catchments are affected (orange circles in Figure 6a), with an
506 average error of 10%.

507 As a further test, we also add bias equal to the mean value to both rainfall and streamflow
508 time series to represent time series affected by systematic bias. If a time series does not have
509 any missing values, adding bias does not generate any variation in the Tr estimate. Missing
510 values in the time series produce discontinuities in the moving averaging process which
511 might lead to small errors. Adding bias equal to the mean value only affected Tr estimates
512 from 6 out of 98 catchments, with an average error of less than 2% (Figure 6b). With this test
513 we show that if additional bias does not significantly alter the shape of the cumulative time
514 series (i.e. the bias is systematic), its effect on Tr estimates is minimal. If the bias is non-
515 systematic its magnitude has still to be big enough to move significantly the centres of mass
516 at window scale to generate any difference in the Tr estimate.

517

518 **Figure 6:** a) Tr estimates using the original time series (black triangles), and adding Gaussian noise with standard deviation equal to 5% the
519 mean value (green stars), or with standard deviation equal to 25% the mean value (orange circles). Often the three markers overlap meaning that
520 there is not difference among the three estimates. b) Tr estimates using the original time series (black triangles), and systematic bias equal to the
521 mean time series value with standard deviation (magenta circles).

522 5.Discussion

523 5.1. Comparison between the DMCA-based and traditional method.

524 Event based estimates of T_r from the proposed DCMA methodology are similar to those
525 found from the traditional method. There are only two catchments which show significant
526 differences in the median T_r values using the two methodologies (see catchment labelled with
527 A (NRFA ID: 40011) and B (NRFA ID: 54008) in Figure 4a). From manually inspecting the
528 events on which the estimates have been produced, the DMCA-based methodology seems to
529 give more realistic estimates. This is also confirmed by the similarity of the DMCA-based
530 estimates with the lag estimates computed for those catchments using the FEH guidelines
531 (Bayliss, 2008; Houghton-Carr, 2008) (see Supporting Information, Table S1). In fact, for
532 catchment A, the lag estimate according to FEH guidelines is around 14 hours (19 hours for
533 DMCA and 2 hours using the traditional method) while for catchment B is around 16 hours
534 (17 hours for DMCA-based and 6 hours using the traditional method). The similarity between
535 T_r estimates with DCMA-based method and lag estimates using FEH guidelines suggests
536 DMCA-based estimates are more likely reliable than that obtained from the traditional
537 method in these sites.

538 The reason why the traditional method performs worse in those catchments is related to the
539 definition upon which the method is built. As pointed out by McCuen (2009), the end of
540 rainfall excess and the inflection point in the hydrograph are both based on individual
541 features and uncertainty in their estimates is generally higher than for average values.
542 Consequently, when the sample is relatively small, this uncertainty can affect the median
543 value. The DMCA-based methodology has the advantage of computing T_r considering the
544 centre of mass of rainfall and streamflow at the scale of the moving average window.

545 When looking at the 25th and 75th percentiles of the distributions we can clearly see that both
546 methods find variability in the T_r estimate across different events. This is not surprising as
547 many studies suggested that the response time of a catchment is a function of the excess
548 rainfall or rainfall intensity (Michailidi et al., 2018; Kjeldsen et al., 2016; Izzard, 1946;
549 Morgali & Linsey, 1965; Askew, 1970; Papadakis & Kazan, 1987; Loukas & Quick, 1996).
550 However, ranges of variability coming from the two methods seem to be visually comparable
551 for most of the catchments, meaning that not only the median values but also the distributions
552 are similar. When ranges for the traditional method are wider it is usually because the method
553 is based on the estimates of extreme features in the hyetograph and hydrograph (e.g.
554 catchment C (NRFA ID: 11004) in Figure 4a). Because the T_r estimates from DMCA-based
555 method are based on centres of mass and hence more stable, we suggest that larger ranges in
556 DMCA-based distribution are instead representative of the actual variability. In fact, unlike
557 the traditional method which searches for the inflection point within a time window following
558 the end of the rainfall, the DMCA-based method is free to search for the actual response
559 having effectively no constraints. The maximum window length tested is set far larger than
560 the expected time scale and therefore this method could cope also with more “unexpected”
561 responses (e.g. catchment D (NRFA ID: 37005) in Figure 4a).

562 One of the main advantages of using the DMCA-based method compared to the traditional
563 method and the other methods summarized by McCuen (2009) is that it avoids the highly
564 uncertain hydrograph separation (Eckhardt, 2008). The T_r estimates from the traditional
565 method and other methods summarized by McCuen (2009) are dependent on the choices

566 made at the baseflow separation stage, while the DMCA-based method is more objective as it
567 does not require any user decision.

568 Another significant advantage of using the DMCA-based methodology is that it does not
569 make any assumption about the rainfall-runoff transformation unlike the currently used
570 methodologies (e.g. the traditional method assumes that the volume of direct runoff is equal
571 to the volume of excess rainfall in the associated hyetograph). Recent results from tracer
572 studies (e.g. McDonnell, 1990; Berghuijs & Allen, 2019; Gallart et al., 2020) have also
573 shown weaknesses about our understanding of rainfall-runoff transformation, so in this sense,
574 the DMCA-based methodology could be an effective tool to estimate the response of the
575 catchment even when assuming that the precipitation which is building the hydrograph is not
576 only the precipitation fallen during the last rainfall event.

577 **5.2. DMCA-based method at event scale and on continuous time series.**

578 Despite the general good agreement between median estimate from individual events and the
579 estimate using the entire time series, it seems that the median value of the individual events
580 lead to larger response times compared to the full time series analysis (Figure 4b). The reason
581 might be that the T_r estimate on full time series gives more weight to bigger floods as they
582 generate a larger portion of negative bivariate fluctuations. In fact, bigger floods seem to
583 show smaller T_r , as the median Spearman rank correlation value between magnitude of the
584 peak and T_r across the 76 catchments is equal to -0.54. This relationship is supported by
585 many studies which show that the response time of a catchment decreases with increasing
586 rainfall or effective rainfall intensity (Michailidi et al., 2018; Kjeldsen et al., 2016; Izzard,
587 1946; Morgali & Linsey, 1965; Askew, 1970; Papadakis & Kazan, 1987; Loukas and Quick,
588 1996). As a result, the T_r estimates from DMCA-based method applied to entire time series
589 cannot be considered an upper limit of the time needed to respond, as intended by the
590 glossary definition (W.M.O., 1974; Johansson, 1984), but it could be particularly useful for
591 engineering applications where usually bigger floods are the ones of interest.

592 It is important to note that by applying the methodology to the time series we avoid the event
593 selection step, which is not standardized (Merz & Blöschl, 2009; Tarasova et al., 2018; Mei
594 & Anagnostou, 2015), and is recognized to affect the statistics at the event scale (Dunkerley,
595 2008). Unlike the traditional method, the DMCA-based methodology applied to the full time
596 series, not only avoids the baseflow separation but also removes the uncertainty around the
597 event selection step by processing the entire time series at once. Therefore, the method can be
598 considered as more objective, since it removes the three biggest sources of uncertainty arising
599 from the application of the methods summarized by McCuen (2009) listed in the introduction
600 section (selection of events, baseflow separation, estimate of hyetograph/hydrograph
601 characteristics).

602 For the reasons explained in the paragraph above and because the method considers a large
603 number and types of events though the use of the entire record, the DMCA-based
604 methodology could be useful for a robust calibration of empirical formulae. Instead, methods
605 summarized by McCuen (2009), which require an event-by-event procedure, could make
606 difficult to consider a significant number of events which also show a variety of different
607 characteristics (Grimaldi et al., 2012; Gericke & Smithers, 2014).

608 **5.3. Robustness analysis of DMCA-based method.**

609 By breaking down time series in sub-datasets of 2, 5 and 10 years (Figure 5), we find that
610 catchments with quicker response times require shorter record lengths for reliable T_r
611 estimate. The reason might be very simple: when a catchment is slow in responding, over a
612 given time period we are able to observe fewer events in comparison to catchments with
613 quicker response times. Although the methodology works on the whole record, the sections
614 of the records important for the T_r estimate are the ones when the streamflow is responding to
615 the rainfall. Therefore if you consider an equal record length in catchments which respond
616 both quickly and slowly to rainfall, in a slow responding catchment these sections are fewer
617 than in a faster responding one because the slow catchment tends to cumulate more rainfall
618 over time in a single response.

619 From this analysis we can conclude that, unless the record is too short compared to the
620 average response time of the catchment, the DMCA-based method is not sensitive to sample
621 size effects as minimum-maximum T_r ranges computed with different n -year sub-datasets are
622 quite narrow. The lengths of the records examined herein can be considered fairly short.
623 Therefore, the method can probably be successfully applied also in catchments for which
624 long records are not available. However, the above conclusion could change in different
625 climates. For example, in arid climates the frequency of the events could be so low that we
626 might need a very long record for a robust estimate of T_r . Therefore, we can consider the
627 results about robustness to short record valid for wet climates only and further testing will be
628 needed in other climatic regions.

629 Furthermore, we show that the proposed method for estimating T_r is robust to noise (Figure
630 6a) and systematic bias (Figure 6b) within the time series. This means that we could apply
631 this methodology even if rain gauge data are not available and we need to make use for
632 example of radar rainfall estimates. Radar rainfall estimates, due to the process of retrieving
633 rainfall intensities from a signal, are more susceptible to noise and bias (Fabry, 2015). These
634 are usually corrected using specific algorithms (e.g. Chumchean et al., 2006) but there might
635 be still some residual errors. However, with the noise and bias tests we showed that T_r
636 estimates using the DMCA-based method would be only minimally affected by slightly
637 inaccurate time series.

638 Overall, the DMCA-based methodology is demonstrated to be robust with respect to
639 relatively short records and presence of artificial noise and bias. For the traditional method a
640 similar analysis could be performed only on an event basis, hence the results would be
641 strongly affected by the decision made at event selection, separation of the hydrograph and
642 estimation of features stages. Therefore, it would be difficult to assess the actual impact of
643 noise and bias because algorithms would require adjustments (e.g. when looking at noisy
644 time series, we would probably need to apply a strong smoothing function to the streamflow
645 time series to find the inflection point in the hydrograph).

646 **6.Summary**

647 Current methodologies to estimate T_r from observed hyetograph and hydrograph show
648 weaknesses in their assumptions and require uncertain and subjective steps. Therefore, we
649 recommend the use of the DMCA-based methodology to estimate the T_r (Python and Matlab
650 code available at https://github.com/giuliagiani/Tr_DMCA, last access 11.09.2020). This

651 method removes many of the sources of uncertainty which affect the existing methods. The
652 DMCA method makes no hypothesis about the rainfall-runoff transformation, avoiding also
653 the uncertain step of hydrograph separation. Furthermore, no selection of rainfall-streamflow
654 events or any parameter estimation are required.

655 The proposed methodology produces estimates of response time that match the ones from the
656 traditional method, showing that the time scale retrieved can be treated as T_r . When applied
657 to the entire time series at once (the intended application) the DMCA-based methodology is
658 easily reproducible as it does not require any user decision. We also show the method is
659 robust to relatively short record lengths, artificial noise and bias within the time series. It is
660 important to note that the DMCA method fully relies on the quality of the data and processing
661 the entire time series at once makes it more difficult to spot anomalous records (although the
662 influence of an individual event is limited, if we have a sample of many events). Hence, it is
663 important that data are quality checked, especially for timing errors. Moreover, another
664 limitation of this method (as many others) is that the proposed method does not provide a
665 physical explanation of the retrieved time parameter.

666 In this paper we have shown the application of the DMCA-based methodology to estimate T_r
667 using hourly time series. This could be particularly useful for a more robust calibration of
668 empirical formulae and for other engineering applications such as designing hydrographs for
669 assigned return periods. Note that our method does not conflict with the hypothesis that
670 hydrographs may incorporate water that fell in previous events. Furthermore, the
671 methodology can be applied at coarser or finer temporal resolutions as long as the temporal
672 resolution of the data is high enough to capture the time delay between the two time series
673 (e.g. no streamflow peak recorded at the same time step of the associated rainfall peak).
674 However, the coarse temporal resolutions may be less informative. For example, in the same
675 set of catchments analysed in this work, daily rainfall and streamflow records would have
676 provided estimates of T_r equal to 1 day for most of the sites, showing that daily data for these
677 predominantly small catchments contains little information on flood event response times.

678 We also suggest that this methodology might be useful for other applications than the
679 estimation of T_r . As long as the temporal resolution of the data is suitable for capturing the
680 phenomena, the DMCA-based method can be used to estimate the response time of any
681 variable to a system driver (e.g. response time of the Biochemical Oxygen Demand
682 concentration in the water when a new rainfall event occurs, or response time of river flow to
683 a snowmelt event).

684 **Acknowledgements**

685 This work is funded as part of the Water Informatics Science and Engineering Centre for
686 Doctoral Training (WISE CDT) under a grant from the Engineering and Physical Sciences
687 Research Council (EPSRC), grant number EP/L016214/1. Information about the U.K.
688 Benchmark Network can be obtained from the website ([https://nrfa.ceh.ac.uk/benchmark-
689 network](https://nrfa.ceh.ac.uk/benchmark-network)). Hourly streamflow time series are available on request from Environmental
690 Agency (EA), Natural Resources Wales (NWR) and Scottish Environmental Protection
691 Agency (SEPA). CEH-GEAR1hr precipitation data are available from the website
692 (<https://doi.org/10.5285/d4ddc781-25f3-423a-bba0-747cc82dc6fa>). Catchment descriptors
693 were taken from the UK Hydrometric Register
694 (http://nora.nerc.ac.uk/id/eprint/3093/1/HydrometricRegister_Final_WithCovers.pdf) and

695 from Bayliss, A. (2008). Our thanks go to Gemma Coxon for help in data preparation and to
696 Lina Stein, Charles West and Sebastian Gnann for the comments on this manuscript. We
697 thank also Riccardo Rigon and other two anonymous reviewers for reviewing this
698 manuscript.

699 **References**

- 700 Almeida, I. K., Almeida, A. K., Anache, J. A. A., Steffen, J. L., & Sobrinho, T.A. (2014).
701 Estimation on time of concentration of overland flow in watersheds: a review. *Geociências*,
702 33(4), 661-671.
- 703 Askew, A.J. (1970). Derivation of formulae for variable lag time. *Journal of Hydrology*, 10
704 (3), 225–242.
- 705 Asquith, W. H., Roussel M. C., Thompson D. B., Cleveland T. G., & Fang X. (2005).
706 *Summary of dimensionless Texas hyetographs and distribution of storm depth developed for*
707 *Texas Department of Transportation Research Project 0-4914*. Austin, Texas: U.S.
708 Geological Survey, Report 0-4194-4.
- 709 Bayliss, A. (2008) *Catchment descriptors*. Flood Estimation Handbook, Vol. 5, Centre of
710 Ecology and Hydrology, Wallingford, UK.
- 711 Berghuijs, W. R., & Allen, S. T. (2019). Waters flowing out of systems are younger than the
712 waters stored in those same systems. *Hydrological Processes*, 33, 3251-3254.
- 713 Beven, K. J. (2020). A history of the concept of time of concentration, *Hydrology and Earth*
714 *System Sciences*, 24, 2655–2670.
- 715 Bracken, L. J., Cox, N. J., & Shannon, J. (2008). The relationship between rainfall inputs and
716 flood generation in south-east Spain. *Hydrological Processes*, 22, 683-696.
- 717 Chow, V. T., Maidment, D. R., & Mays, L. W. (1988). *Applied hydrology*. New York:
718 McGraw-Hill.
- 719 Chumchean, S., Sharma, A., & Seed, A. (2006). An integrated approach to error correction
720 for real-time radar rainfall estimation. *Journal of Atmospheric and Oceanic Technology*, 23,
721 67-79. Dunkerley, D. (2008). Identifying individual rain events from pluviograph records: a
722 review with analysis of data from an Australian dryland site. *Hydrological Processes*, 22,
723 5024-5036.
- 724 Dooge, J.C.I. (1973). *Linear theory of hydrologic systems*. US Department of Agriculture,
725 Technical Bulletin 1468.
- 726 Eckhardt, K. (2005). How to construct recursive digital filters for baseflow separation.
727 *Hydrological Processes*, 19 (2), 507-515.
- 728 Eckhardt, K. (2008). A comparison of baseflow indices, which were calculated with seven
729 different baseflow separation methods. *Journal of Hydrology*, 352(1), 168-173.
- 730 Fabry, F. (2015). *Radar Meteorology: Principles and Practice*. Cambridge University Press.
- 731 Furey, P.R., & Gupta, V.K. (2001). A physically based filter for separating baseflow from
732 streamflow time series. *Water Resources Research*, 37(11), 2709-2722.
- 733 Gallart, F., von Freyberg, J., Valiente, M., Kirchner, J., Llorens, P., & Latron, J. (2020).
734 Technical note: An improved discharge sensitivity metric for young water fractions.
735 *Hydrology and Earth System Sciences*, 24, 1101–1107.
- 736 Gericke, O. J., & Smithers, J. C. (2014). Review of methods used to estimate catchment
737 response time for the purpose of peak discharge estimation, *Hydrological Sciences Journal*,
738 59:11, 1935-1971.

- 739 Grimaldi, S., Petroselli, A., Tauro, F. & Porfiri, M. (2012). Time of Concentration: a paradox
740 in modern hydrology. *Hydrological Sciences Journal*, 57 (2), 217–228.
- 741 Harrigan, S., Hannaford, J., Muchan, K., & Marsh, T. J. (2018). Designation and trend
742 analysis of the updated UK Benchmark Network of river flow stations: The UKBN2 dataset.
743 *Hydrology Research*, 49 (2), 552-567.
- 744 Henderson, F. M. & Wooding, R. A. (1964). Overland flow and groundwater flow from a
745 steady rainfall of finite duration. *Journal of Geophysical Resources*, 69, 1531–1540.
- 746 Houghton-Carr, H. A. (2008). *Restatement and application of the Flood Studies Report*
747 *rainfall-runoff method*. Flood Estimation Handbook, Vol. 4, Centre of Ecology and
748 Hydrology, Wallingford, UK.
- 749 Izzard, C. F., & Hicks, W. I. (1946). *Hydraulics of runoff from developed surfaces*. In: 26th
750 Annual Meetings of the Highway Research Board, 5–8 December, Washington, DC, 129–
751 150.
- 752 Johansson, I. (Ed.) (1984). *Nordic Glossary of Hydrology*, Almquist and Wiksell
753 International: Stockholm.
- 754 Kibler, D. F. (1982). Desk-top methods for urban stormwater calculation. In: *Urban*
755 *stormwater hydrology*, D. F. Kibler (Ed.), American Geophysical Union, Water Resources
756 Monograph 7, Washington, D.C., 87–135. Kjeldsen, T. R., Kim, H., Jang, C., & Lee, H.
757 (2016). Evidence and implications of nonlinear flood response in a small mountainous
758 watershed. *Journal of Hydrologic Engineering*, 21 (8), 04016024.
- 759 Kristoufek, L. (2014). Detrending moving-average cross-correlation coefficient: Measuring
760 cross-correlations between non-stationary series. *Physic A*, 406, 169-175.
- 761 Kristoufek, L. (2015). Power-law correlations in finance-related Google searches, and their
762 cross-correlations with volatility and traded volume: Evidence from the Dow Jones Industrial
763 components. *Physic A*, 428, 194-205.
- 764 Lewis, E., Quinn, N., Blenkinsop, S., Fowler, H. J., Freer, J., Tanguy, M., Hitt, et al. (2018).
765 A rule based quality control method for hourly rainfall data and a 1 km resolution gridded
766 hourly rainfall dataset for Great Britain: CEH-GEAR1hr. *Journal of Hydrology*, 564, 930-
767 943.
- 768 Loukas, A., & Quick, M. C. (1996). Physically-based estimation of lag time for forested
769 mountainous watersheds. *Hydrological Sciences Journal*, 41 (1), 1–19.
- 770 Luce, C. H., & Cundy, T. W. (1994). Parameter identification for a runoff model for forest
771 roads, *Water Resources Research*, 30, 1057–1069.
- 772 Lyne, V., & Hollick, M. (1979). *Stochastic time-variable rainfall-runoff modelling*. Institute
773 of Engineers Australia National Conference, Publ. 79/10, 89-93.
- 774 Marsh, T. J., & Hannaford, J. (Eds) (2008). *UK Hydrometric Register*. Hydrological data UK
775 series. Centre for Ecology & Hydrology, 210 pp.
- 776 McCuen, R. H. (2009). Uncertainty analyses of watershed time parameters, *Journal of*
777 *Hydrologic Engineering*, 14 (5), 490–498.

- 778 McDonnell, J.J. (1990). A rationale for old water discharge through macropores in a steep,
779 humid catchment. *Water Resources Research*, 26, 2821–2832.
- 780 Mei, Y., & Anagnostou, E. N. (2015). A hydrograph separation method based on information
781 from rainfall and runoff records. *Journal of Hydrology*, 523, 636–649.
- 782 Merz, R., & Blöschl, G. (2009). A regional analysis of event runoff coefficients with respect
783 to climate and catchment characteristics in Austria. *Water Resources Research*, 45, W01405.
- 784 Michailidi, E. M., Antoniadis, S., Koukouvinos, A., Bacchi, B. & Efstratiadis, A. (2018).
785 Timing the time of concentration: shedding light on a paradox. *Hydrological Sciences*
786 *Journal*, 63(5), 721-740.
- 787 Morgali, J.R. & Linsley, R.K. (1965). Computer simulation of overland flow. *Journal of*
788 *Hydraulics Division ASCE*, 91 (HY3), 81–100. Nathan, R.J. & McMahon, T.A. (1990).
789 Evaluation of automated techniques for baseflow and recession analysis. *Water Resources*
790 *Research*, 26 (7), 1465-1473.
- 791 Norbiato, D., Borga, M., Merz, R., Blöschl, G., & Carton, A. (2009). Controls on event
792 runoff coefficients in the eastern Italian Alps. *Journal of Hydrology*, 375, 312–325.
- 793 Papadakis, K.N. & Kazan, M.N. (1987). *Time of concentration in small rural watersheds*. In:
794 *Proceedings of the ASCE Engineering Hydrology Symposium*. Williamsburg, VA: ASCE,
795 633–638.
- 796 Perdikaris, J., Gharabaghi, B., & Rudra, R. (2018). Reference Time of Concentration
797 Estimation for Ungauged Catchments. *Earth Science Research*, 7(2), 58-73.
- 798 Sloto, R. A. & Crouse, M. Y. (1996). *HYSEP, a computer program for streamflow*
799 *hydrograph separation and analysis*. US Department of the Interior, US Geological Survey-
800 Resources Investigations Report 1996–4040, 46 p.
- 801 Snyder, F.F. (1938). Synthetic unit-graphs. *Transactions of the American Geophysical Union*,
802 19:447 454.
- 803 Tarasova, L., Basso, S., Zink, M., & Merz, R. (2018). Exploring controls on rainfall-runoff
804 events: 1. Time-series-based event separation and temporal dynamics of event runoff
805 response in Germany. *Water Resources Research*, 54.
- 806 USDA-SCS (US Department of Agriculture – Soil Conservation Service) (1986). *Urban*
807 *hydrology for small watersheds*. Washington, DC: US Department of Agriculture, Soil
808 Conservation Service, Technical release 55.
- 809 USDA-NRCS (US Department of Agriculture – Natural Resources Conservation Service)
810 (2010). *Time of concentration*. Washington, DC: US Department of Agriculture, Natural
811 Resources Conservation Service, Hydrology National Engineering Handbook Part 630.
- 812 W.M.O. (1974). *International Glossary of Hydrology*, W.M.O. Report No. 385: Geneva.
- 813

Figure 1.

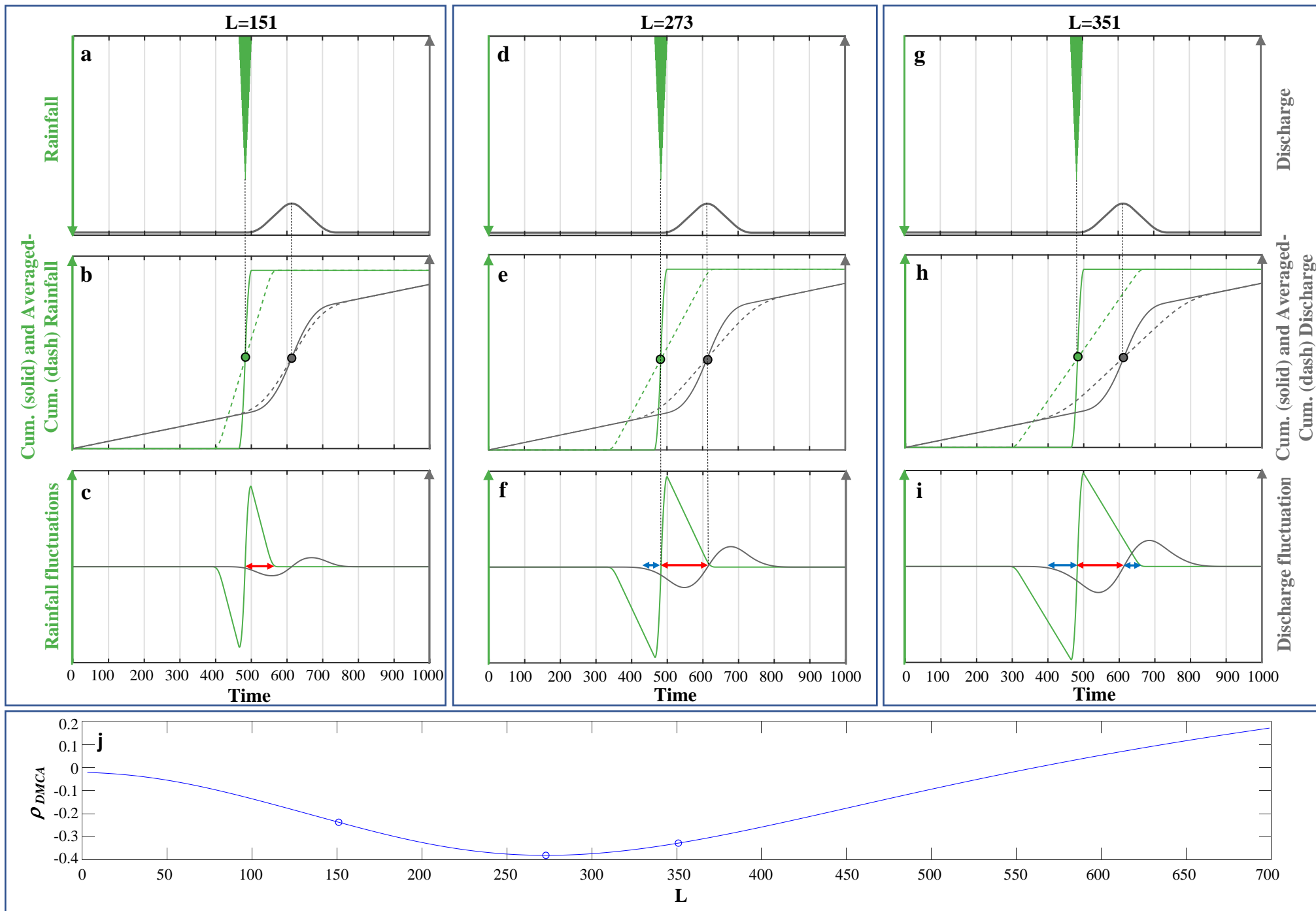


Figure 2.

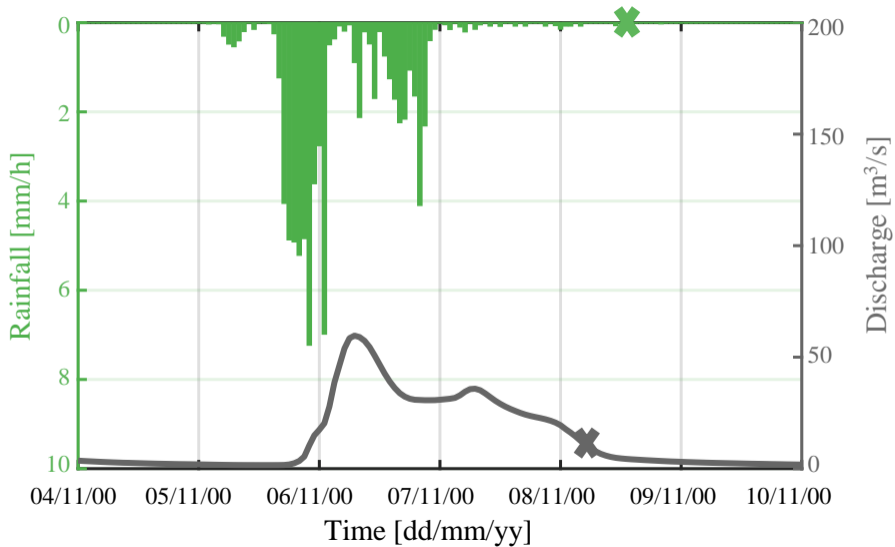


Figure 3.

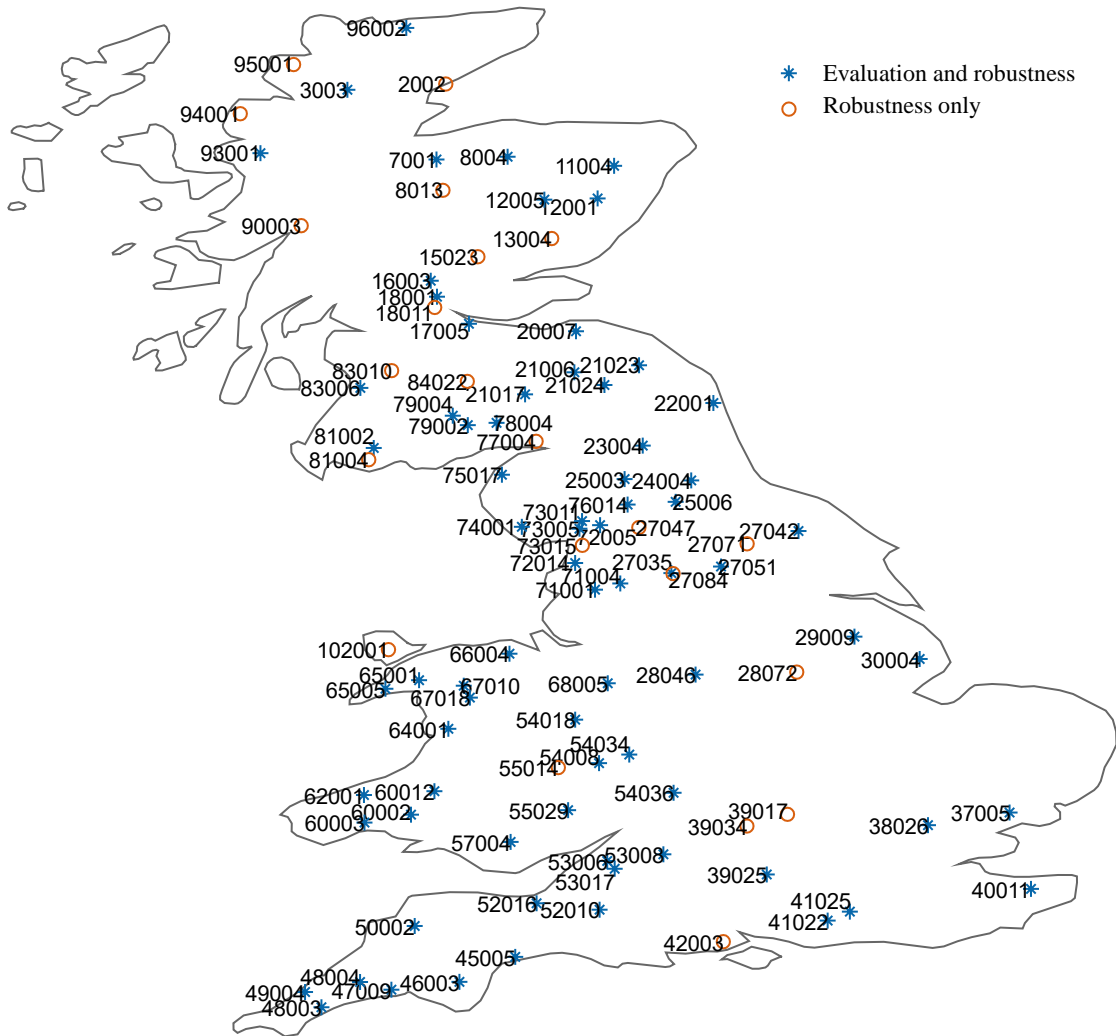
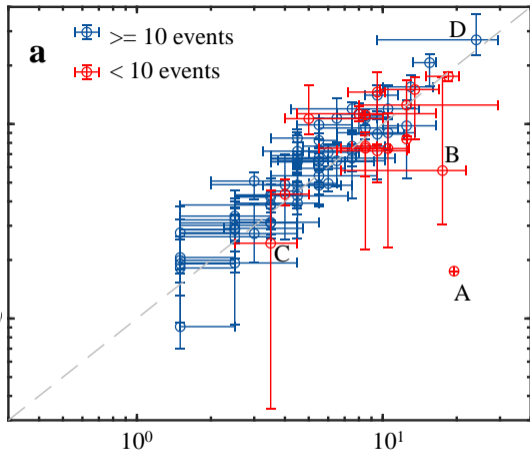


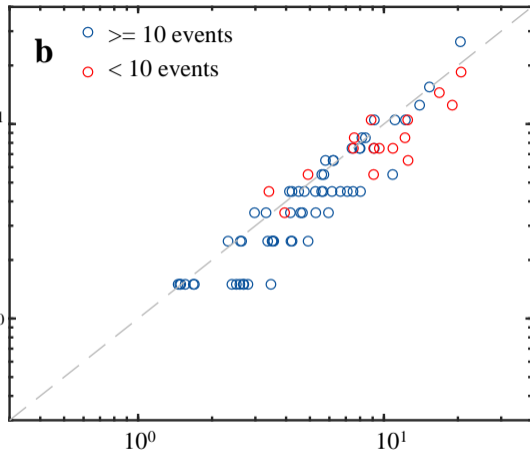
Figure 4.

Tr traditional method - 25th, 50th, 75th
distribution individual events [hours]



Tr DMCA method - 25th, 50th, 75th
distribution individual events [hours]

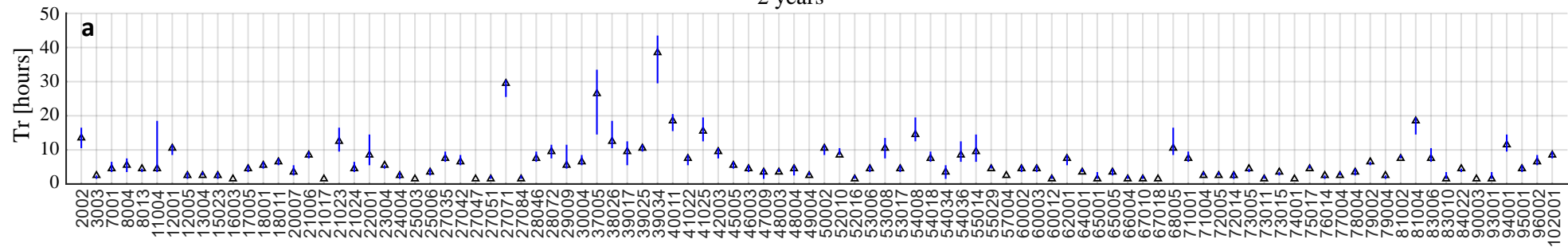
Tr DMCA method - entire timeseries
[hours]



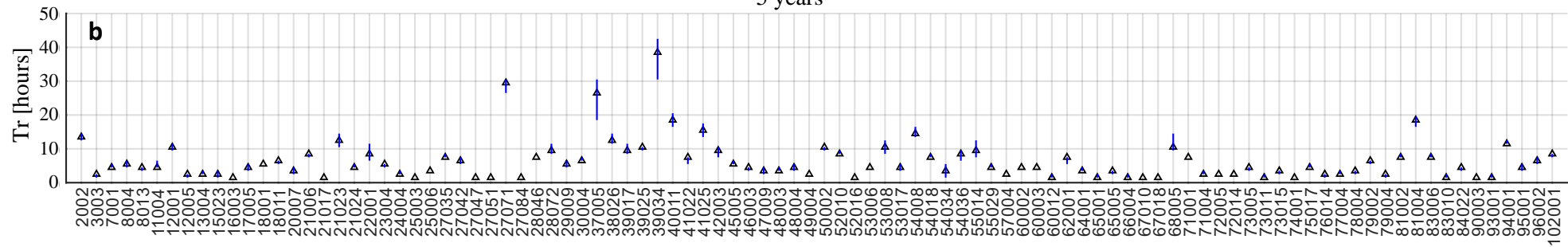
Tr DMCA method - median individual
events [hours]

Figure 5.

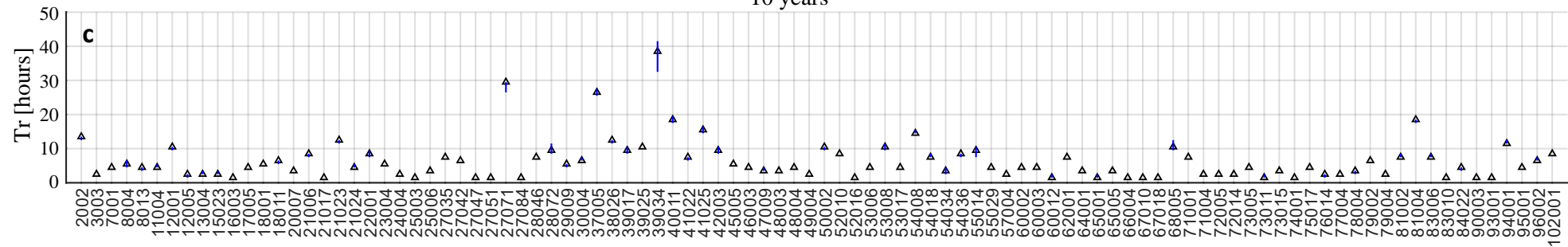
2 years



5 years



10 years



NRFA catchment IDs

Figure 6.

